Powder Metallurgy and Metal Ceramics, Vol. 47, Nos. 7-8, 2008

SINTERED METALS AND ALLOYS

MECHANICAL PROPERTIES OF POWDER TITANIUM AT DIFFERENT PRODUCTION STAGES. I. DENSIFICATION CURVES FOR TITANIUM POWDER BILLETS

E. M. Borisovskaya,[1] V. A. Nazarenko,[1] Yu. N. Podrezov, [1,2] O. S. Koryak,[1] Ya. I. Evich,[1] and V. F. Gorban'[1]

UDC 621.762.4539.217.620.178.015

The mechanical behavior of titanium powder billets at all production stages is examined. The dependence of how mechanical properties are formed on the structure is established. The compaction of a powder pressed in a rigid die mold, which is the initial stage of the production process, is analyzed. The experimental dependence of the compacting force on porosity is examined. The results are compared with theoretical data available.

Keywords: *powder titanium, mechanical properties, strain hardening.*

INTRODUCTION

Titanium is one of the most popular metals since it has many advantages over other metals because, first of all, it combines a small weight and high strength. Titanium metallurgy in general and titanium powder metallurgy in particular are quite difficult as titanium has a great affinity for oxygen. That is why ways to improve the titanium and titanium alloy production process have been sought for many years. There are adequate data on powder metallurgy methods to make titanium products [1], but there has hardly been comprehensive research into the evolution of the structure and properties of titanium billets at all production stages. This cycle of publications proposes analyzing the mechanical behavior of powder titanium billets at all production stages and associates mechanical properties with structural evolution.

This paper examines the first stage of making a powder product: densification in a rigid die mold. Relating the compaction pressure to porosity is very important both for powder metallurgy theory and actual production of powder parts with preset properties.

There are a lot of publications that analyze the densification and propose analytical connection between the compaction force and porosity. These publications are either of formal phenomenological nature (e.g., the theory of Bal'shin and his followers [2–4]) or are based on the analysis of physical processes that occur in solids when deformed [5–7]. The authors of these publications note, as a rule, that densification proceeds in stages. Practically strain-free motion of particles prevails at the first stages, the near-surface areas of the powder particles become

[1]Institute for Problems of Materials Science, National Academy of Sciences of Ukraine, Kiev, Ukraine.
[2]To whom correspondence should be addressed; e-mail: podrezov@materials.kiev.ua.

Translated from Poroshkovaya Metallurgiya, Vol. 47, No. 7–8 (462), pp. 43–52, 2008. Original article submitted February 22, 2007.

 1068-1302/08/0708-0406 ©2008 Springer Science+Business Media, Inc.

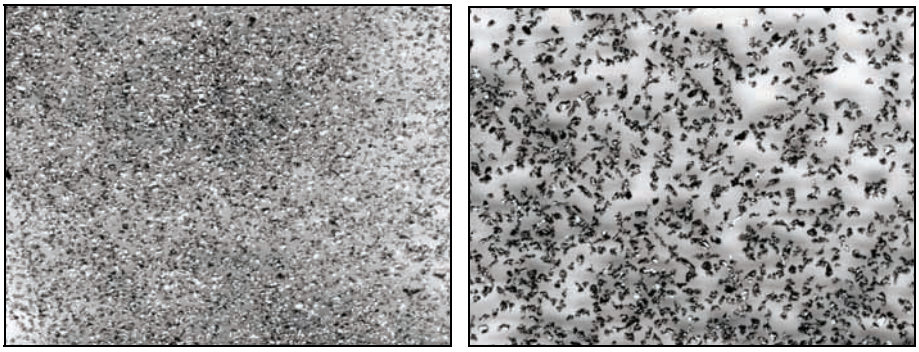

a *b*

Fig. 1. Titanium powder of fine (*a*) and coarse (*b*) fractions

deformed when pressure increases, and plastic deformation occurs in the volume of particles in further densification.

It is plastic deformation of powder particles that is paid special attention in this paper. The point is that most publications do not allow for the mechanisms of solid-phase hardening, which predetermine the compressibility along with the evolution of pore morphology. The authors have gained wide experience in examining the densification of commercially pure recrystallized and deformed titanium [8, 9], which permits a deeper insight into the densification of powder titanium billets.

MATERIALS AND PROCEDURE

In this paper, as well as in all subsequent papers of this cycle, titanium powder of PTÉS grade was used to produce samples. The powder was bolted into the following fractions: –063; –063+05; –05+0315; –0315+02; –02+01. Table 1 summarizes the properties of the initial powders. Figure 1 shows fine and coarse powder fractions to give an idea of the initial particle shape.

TABLE 1. Properties of Initial Titanium Powders

Fraction	Density, g/cm^3		Hausner factor $I = \rho_c/\rho_b$	Yield, sec
	Bulk	Compacted		
–063	1.34	1.68	1.25	30.9
–063+05	1.32	1.58	1.20	36.5
–05+0315	1.31	1.63	1.24	33.3
–0315+02	1.32	1.63	1.23	30.0
–02+01	1.24	1.58	1.28	29.8

TABLE 2. Porosity of Samples Depending on Compressibility of Titanium Powder of Different Fractions

P, MPa	Fraction				
	–063	–063+05	–05+0315	–0315+02	–02+01
100	41.19	39.95	40.34	40.35	42.23
200	31.00	29.94	30.17	29.09	33.22
400	20.31	19.10	19.77	18.24	22.12
600	14.21	14.26	14.10	14.51	15.60
800	10.25	9.89	9.87	10.60	11.72

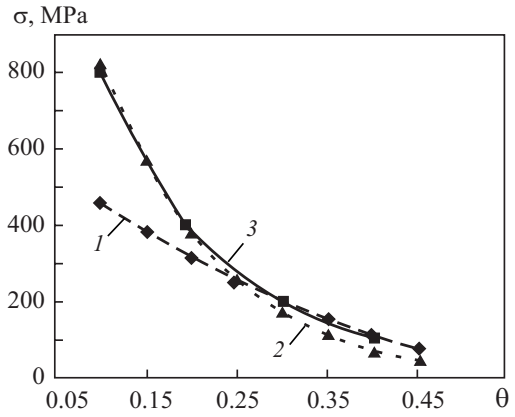

Fig. 2

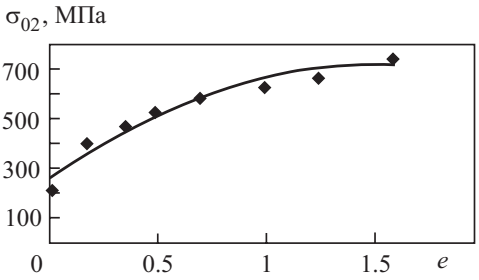

Fig. 3

Fig. 2. Densification curves of powder titanium: *1*) T1 [7, 16], *2*) T2 [11], *3*) experimental results

Fig. 3. Yield stress as a function of titanium strain: the dots stand for experimental values and the curve for values fitted by Eq. (1)

Samples of two types were made of each powder fraction by cold double-action pressing for mechanical tests: cylinders 9.6–14.7 mm in height and 11 mm in diameter for Brazilian test and uniaxial compression; parallelepipeds 5 × 7 × 45 mm for four-point bending tests. Compaction stress was recorded during pressing, and the porosity of the samples was measured after that.

Table 2 summarizes these parameters for the cylindrical compacts. The values of porosity are averaged for 10 samples compacted under the same pressure. The porosity of the compacts somewhat increases with decreasing powder particle sizes (Table 2).

EXPERIMENTAL RESULTS

This paper is concerned with densification curves plotted in stress σ–porosity θ coordinates (Fig. 2) and analytical description of this dependence.

A densification curve for compacted material can be regarded as a variety of a strain-hardening curve. As different from compact material, the strain coordinate is associated with changes in porosity since deformation is due to changes in volume, but not changes in shape. The stress coordinate (as in the case of compact material) characterizes the stress needed for solid-phase flow. For a porous body, this stress is determined by the presence of pores, which govern the distribution of stresses. It is obvious that deforming stress in compact material needs to be adequate to overcome the resistance from all structural elements with moving dislocations.

To determine how the yield stress depends on the strain in deformed titanium, we conducted a series of additional experiments on VT1-0 compact titanium samples that had been deformed to reach different strains. We examined the hardening parameters in the compression of titanium deformed by rolling to strain $e = 0.2–1.7$ in three mutually perpendicular directions denoted by *X*, *Y*, and *Z* (Table 3).

We used the values of yield stress averaged for the three directions to plot a strain-hardening curve for titanium (Fig. 3). According to the hardening theory proposed by Ludwig, this curve is described by the exponential function $\sigma_y = \sigma_0 + Ke^n$, where σ_0 is the yield stress of undeformed material; *K* is hardening factor; and *n* is strain-hardening index.

The experimental dependence of deforming stress on strain is well fitted by the following expression:

$$\sigma_y = \sigma_0 + Ke^{0.7}, \quad (1)$$

where $\sigma_0 = 270$ MPa; $K = 380$ MPa.

Assuming that powder-phase deformation to the equivalent strain (calculated through changes in density) needs the same force as compact material does, we can regard the curve in Fig. 3 as the basis for plotting the densification curve.

TABLE 3. Hardening Parameters of Predeformed Titanium Tested by Uniaxial Compression

Deformation direction	Stress σ_y, MPa, at strain e							
	0	0.18	0.36	0.5	0.7	1.0	1.25	1.7
σ_y (X)	270	418	565	570	640	615	607	705
σ_y (Y)	270	395	647	630	620	655	705	700
σ_y (Z)	270	470	595	610	573	730	760	860

The equivalent strain in the densification of a porous body was calculated in many papers [10–17]. The equivalent strain–porosity expressions fundamentally differ from various loading patterns [15–17]. We potted the densification curve using the model proposed in [11], which is most close to the densification in a die mold. In this case, the stress tensor is calculated as follows:

$$\sigma = -\frac{2(1-\theta)\sigma}{3}\sqrt{\frac{1-\theta}{\theta}}. \tag{2}$$

The σ corresponds to the yield stress in the solid phase in equivalent strain. The strain is described as follows:

$$e = \frac{4}{3}\left(\operatorname{arctg}\sqrt{\frac{\theta_0}{1-\theta_0}} - \operatorname{arctg}\sqrt{\frac{\theta}{1-\theta}}\right), \tag{3}$$

where θ and θ_0 are current and initial porosities, respectively. In the case in question, θ_0 is the ultimate porosity of the compact associated with its bulk density with the following relation: $\theta_0 = (\rho - \rho_c)/\rho$.

We solve Eqs. (1)–(3), simultaneously to plot the densification curve T2 (Fig. 2). This dependence agrees well with the experimental results for low and medium porosity, but gives underestimated values for high porosity. We think that this deviation from the experimental results is due to changes in the stress-strain state of the compact.

Based on our experimental data [7] and Koval'chenko's calculations [19, 20], the effective Poisson ratio in uniaxial loading tends to zero at a porosity of about 30%. Therefore, there is no lateral pressure on the compact from the die mold at high porosity because of small transverse strain, and the sample is pressed in conditions that correspond to uniaxial compression.

According to [7], we can calculate the stress developed in a porous sample in this case using the similarity principle for densification curves, which states that the yield stresses of compact and porous materials are in the same ratio as their elastic moduli are. The relation of yield stress on porosity is expressed by the following exponential function [21]:

$$\sigma_y(\theta) = \sigma_y^c(1 - \theta/\theta_0)^{1.65}, \tag{4}$$

which represents the modified Bal'shin equation considering that the ultimate porosity θ_0 of the compact corresponds to its bulk density. (Here σ_y^c is the yield stress of the solid phase.)

If transverse sizes of the sample remain unchanged (the efficient Poisson ratio being $\nu = 0$), the strain of high-porous materials is associated with their porosity with the following relation [22, 23]:

$$e = (\theta_0 - \theta)/(1 - \theta). \tag{5}$$

If the Poisson ratio is negative in the deformation of high-porous materials [19], the relation between their porosity and strain is described by the expression for triaxial compression:

$$e = 4/3[(\theta_0)^{1/2} - (\theta)^{1/2}]. \tag{6}$$

Note that Eqs. (5) and (6) give close values of strain over the entire porosity range. Solving Eqs. (1), (4), and (6) simultaneously, we obtain the densification curve denoted by T1 in Fig. 2. Comparing the theory and experiment shows that the calculated compaction stress at high porosity agrees well with the experimented data. With increasing density of the compact, the experimental data become somewhat higher that the calculated ones

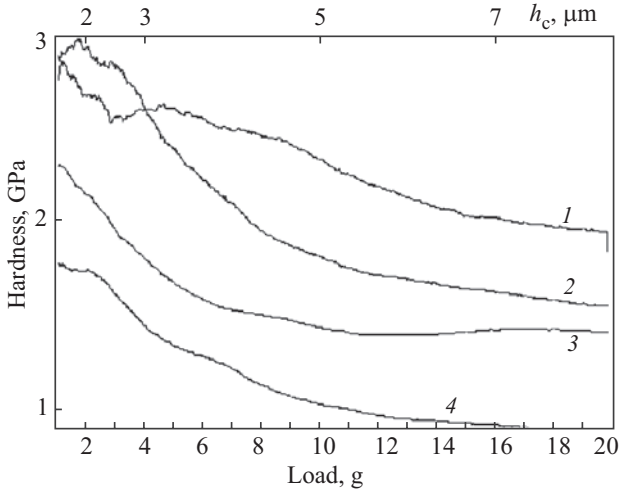

Fig. 4. Hardness as a function of indentation depth h_c in continuous-indentation experiments

since the proposed procedure to plot a densification curve accounts only for the stresses developed in the solid phase and ignores the lateral pressure from the die mold.

Hence, in denser states, when the lateral pressure from the die mold additionally contributes to hardening, the densification curve is more accurately described by the model proposed in [11]. In the densification of high-porous materials, when the transverse sizes of the compact remain practically unchanged, the other calculation procedure provides more accurate results.

DISCUSSION OF RESULTS

The proposed approach to plotting the densification curve assumes that the densification parameters for deformed compact material and the powder phase of porous material compacted to the same equivalent strain should be similar. To verify this assumption, we compared the yield stress of deformed compact material with the hardness of individual powder particles, H_μ. According to the theory that associates yield stress with hardness, the relation $H_\mu/3 = \sigma_y$ applies well to deformed materials [24–26].

Figure 4 shows hardness curves for deformed powder particles across the depth of indentation when hardness is measured by continuous-indentation method. The experimental results summarized in Table 4 indicate that the $H_\mu/3$ values for the central part of a powder particle are practically the same as σ_y of the compact sample deformed to the same equivalent strain. The form of the hardness–indentation depth dependence indicates that strain is distributed more uniformly over a powder particle in denser compacts than in porous ones in which it is mainly concentrated in near-surface layers. Hence, the hardness of high-porous compacts changes from the surface deep into the powder particle (Fig. 4, curves *2*, *3*). Therefore, comparing the densification parameters for the solid phase of compacts with the properties of deformed titanium shows good agreement between theory and experiment.

Note that, in the proposed densification curve analysis, the deforming stress of the solid phase reached in the compact at a given strain is determined from independent experiment performed on compact samples deformed

TABLE 4. Yield Stress of Deformed Titanium and Hardness of Powder Particles after Pressing

Compact porosity, %	e_{eq}	σ_y, MPa	H_μ, MPa	H_μ/σ_y
40.28	0.281	495	1000	2.02
30.62	0.377	582	1600	2.74
20.03	0.525	619	1700	2.75
9.95	0.714	630	1950	3.09

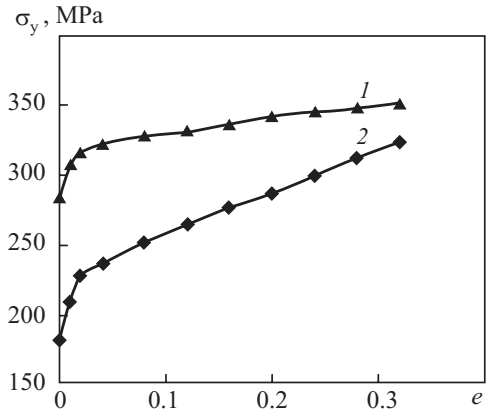

Fig. 5. Hardening curves for titanium samples: *1*) deformed state (e = 0.7); *2*) compact with 20% initial porosity

to different strains. The papers that focus on the densification of brittle loose media [12] and plastic powder metals [13] often use results from uniaxial compression tests of densified compacts to calculate the deforming stress. It is assumed in these cases that the fracture stress [14] or yield stress [15] of the compact being compressed correlates with the stresses developed in material being densified.

The difference in the mechanical behavior of deformed compact titanium tested by uniaxial compression and of the compact deformed to the same strain is revealed when the strain-hardening curves of these materials are analyzed. Figure 5 represents curve *2* showing the hardening of the compact densified to a porosity of 20%, which corresponds, according to Eq. (3), to equivalent strain e = 0.7, and curve *1* showing the strain hardening of compact titanium pre-deformed to e = 0.7, which (to account for the effect of porosity on hardening) has been normalized to the coefficient derived from Eq. (4) for a porosity of 20%. While deformed titanium has very low hardening parameters because of the features of dislocation structure that we described in [8], the green compact deformed to the same equivalent strain has much lower yield stress and densifies much faster. The high densification parameters of the compact are most likely associated with the evolution of pore space, but not with special mechanisms by which the solid phase of the compact hardens. The pore morphology formed in pressing is noticeably distorted when the sample is unloaded due to elastic after-effect. When the sample is repeatedly loaded, plastic strain is not uniform on different surfaces. This process turns to be "smeared out" by strain, which decreases the effective yield stress, on the one hand, and increases the effective hardening parameters, on the other.

The densification curves resulting from uniaxial compression tests of porous compacts do not agree so well with the experimental data. In particular, the yield stress of the green compact is several times lower than the pressing stress over the entire porosity range of interest. The fracture stress of high-porous compacts is also substantially lower than the pressing stress, and compacts with a porosity lower than 20% don not break in compression at all.

Therefore, the results show that the stresses developed *in situ* in the compact when densified and *post factum* when repeatedly loaded (e.g., by uniaxial compression) substantially differ because the pore space of the compact evolve in response to elastic after-effect.

CONCLUSIONS

A densification curve for commercially pure powder titanium has been plotted experimentally and theoretically with account of the solid-phase densification and pore-space evolution. The theory and experiment are in good agreement.

In the densification of high-porous materials, when the transverse sizes of the compact remain practically unchanged, calculation with the model [7] is more accurate. In denser states, when lateral pressure from the die

mold additionally contributes to hardening, the densification curve is more accurately described with the model proposed in [11].

The continuous-indentation method is used to analyze how hardness changes across the depth of powder particles in compacts with different porosity. It is established that strain is distributed more uniformly across the powder particle in dense compacts than in porous ones in which it is mainly concentrated in near-surface layers. Hence, hardness abruptly changes from the surface deep into the powder particles in high-porous compacts.

Comparing the hardening curves for compact deformed titanium and a compact deformed to the same equivalent strain shows that the compact has much lower yield stress but much higher hardening coefficient. This is attributed to the evolution of the pore space when the compact is repeatedly loaded.

REFERENCES

1. V. S. Ustinov, Yu. G. Olesov, L. N. Antipin, and V. A. Drozdenko, *Powder Metallurgy of Titanium* [in Russian], Metallurgiya, Moscow (1973).
2. M. Yu. Bal'shin, *Powder Physical Metallurgy* [in Russian], Metallurgizdat, Moscow (1948).
3. G. M. Zhdanovich, *Pressing Theory of Metal Powders* [in Russian], Metallurgiya, Moscow (1969), p. 264.
4. M. Yu. Bal'shin, N. V. Zakharyan, and N. V. Manukyan, "Calculation of the relationship between compaction pressure and the density of metal powders," *Powder Metall. Met. Ceram.*, **12**, No. 5, 372–375 (1973).
5. R. W. Heckel, "Advanced experimental techniques in powder metallurgy," in: *Perspectives in Powder Metallurgy*, Vol. 5, New York–London (1970), p. 139.
6. J. L. Bruckpool, *Modern Developments in PM, Vol. 5: Materials and Properties*, New York (1968), pp. 201–216.
7. S. A. Firstov, A. N. Demidik, I. I. Ivanova, et al., *Structure and Strength of Powder Materials* [in Russian], S. A. Firstov and M. Shlessar (eds.), Naukova Dumka, Kiev (1993), p. 175.
8. Yu. N. Podrezov, "Nanocrystalline structure formation under severe plastic deformation and its influence on mechanical properties," *Fiz. Tekh. Vys. Davl.*, **15**, No. 1, 11–18 (2005).
9. S. A. Firstov, Yu. N. Podrezov, N. I. Danilenko, et al., "Roles of relaxation processes in hardening of nanocrystalline materials produced by severe plastic deformation," *Fiz. Tekh. Vys. Davl.*, **13**, No. 3, 37–47 (2003).
10. E. M. Borisovskaya, D. G. Verbilo, V. A. Pisarenko, et al., "Structurization and mechanical properties of deformed titanium," *Fiz. Tekh. Vys. Davl.*, **17**, No. 2, 110–118 (2007).
11. I. F. Martynova, "Physical features of plastic deformation of porous bodies," in: *Rheological Models and Deformation of Porous Powder and Composite Materials* [in Russian], Naukova Dumka, Kiev (1985), pp. 98–105.
12. D. C. Drucker and W. Prager, "Soil mechanics and plastic analysis of limit design," *Quarterly of Applied Mathematics*, **10**, 157–175 (1952).
13. G. Porial, E. Euvrard, P. Tailhades, and A. Rousset, "Relationship between compaction pressure, green density, and green strength of powder compacts used in thermal batteries," *Powder Metal.*, **42**, No. 1, 34–40 (1999).
14. E. Yu. Vyal' and A. M. Laptev, "Strength of unsintered powder compacts with axial and radial loading," *Powder Metall. Met. Ceram.*, **41**, No. 5–6, 249–252 (2002).
15. O Coube and H Riedel, "Numerical simulation of metal powder die compaction with special consideration of cracking, *Powder Metal.*, **43**, No. 2, 123–131 (2000).
16. I. F. Martynova and V. V. Skorokhod, "Densification of porous metal during volume plastic deformation in the absence of work-hardening," *Powder Metall. Met. Ceram.*, **15**, No. 5, 343–345 (1976).
17. V. V. Skorokhod, I. F. Martynova, and V. P. Shklyarenko, "Irreversible deformation of a sintered porous body of a work-hardening plastic metal. II. Experimental part," *Powder Metall. Met. Ceram.*, **16**, No. 5, 369–375 (1977).

18. I. F. Martynova and M. B. Shtern, “An equation for the plasticity of a porous solid allowing for true strains of the matrix material,” *Powder Metall. Met. Ceram.*, **17**, No. 1, 17–21 (1978).
19. M. S. Koval’chenko, “Mechanical properties of isotopic porous materials,” *Powder Metall. Met. Ceram.*, **35**, No. 9–10, 561–568 (1996).
20. M. S. Koval’chenko, “Elasticity and viscosity of isotropic porous materials,” *Powder Metall. Met. Ceram.*, **42**, No. 1–2, 81–87 (2003).
21. Yu. N. Podrezov, A. G. Kostornov, N. I. Lugovoi, et al., “Elastic modulus of highly porous nickel-based materials,” *Powder Metall. Met. Ceram.*, **36**, No. 3–4, 203–206 (1997).
22. Yu. N. Podrezov, L. I. Chernyshev, N. I. Lugovoi, et al., “Effect of the pore space structure in a biporous material on the elastic modulus. Phenomenological analysis,” *Powder Metall. Met. Ceram.*, **33**, No. 11–12, 628–632 (1995).
23. Yu. N. Podrezov, N. I. Lugovoi, V. N. Slyunyaev, and D. G. Verbilo, “Effect of the pore space structure on deformation energy absorption during compression of high-porosity composites. Part I. Low hardening stage,” *Powder Metall. Met. Ceram.*, **39**, No. 7–8, 407–413 (2000).
24. Yu. V. Mil’man, S. I. Chugunova, and I. V. Goncharova, “Indentation analysis of the mechanical behavior of low-plastic materials,” in: *Structure and Properties of Promising Materials*, A. E. Potekaev (ed.), Izd. Nauch. Tekh. Lit., Tomsk (2006), pp. 301–322.
25. B. A. Galanov, Yu. V. Mil’man, S. I. Chugunova, and I. V. Goncharova, “Indentation analysis of the mechanical properties of very hard materials,” *Sverkhtverd. Mater.*, No. 3, 25–38 (1999).
26. Yu. V. Milman, “Plasticity characteristic obtained by indentation,” *J. Physics D: Applied Physics*, **41,** No. 7, 1–9 (2008).